Substituent Effects on the Stability of Thallium and Phosphorus Triple Bonds: A Density Functional Study

Jia-Syun Lu [1], Ming-Chung Yang [1] and Ming-Der Su [1,2,*] (ID)

[1] Department of Applied Chemistry, National Chiayi University, Chiayi 60004, Taiwan; s1022818@mail.ncyu.edu.tw (J.-S.L.); mingchungmc@gmail.com (M.-C.Y.)

[2] Department of Medicinal and Applied Chemistry, Kaohsiung Medical University, Kaohsiung 80708, Taiwan

[*] Correspondence: midesu@mail.ncyu.edu.tw; Tel.: +886-5-2717964

Abstract: Three computational methods (M06-2X/Def2-TZVP, B3PW91/Def2-TZVP and B3LYP/LANL2DZ+dp) were used to study the effect of substitution on the potential energy surfaces of $RTl \equiv PR$ (R = F, OH, H, CH_3, SiH_3, $SiMe(SitBu_3)_2$, $SiiPrDis_2$, Tbt (=C_6H_2-2,4,6-$(CH(SiMe_3)_2)_3$), and Ar* (=C_6H_3-2,6-$(C_6H_2$-2, 4,6-i-$Pr_3)_2$)). The theoretical results show that these triply bonded $RTl \equiv PR$ compounds have a preference for a bent geometry (i.e., $\angle R–Tl–P \approx 180°$ and $\angle Tl–P–R \approx 120°$). Two valence bond models are used to interpret the bonding character of the $Tl \equiv P$ triple bond. One is model [I], which is best described as $Tl \leftrightarrows P$. This interprets the bonding conditions for $RTl \equiv PR$ molecules that feature small ligands. The other is model [II], which is best represented as $Tl \equiv P$. This explains the bonding character of $RTl \equiv PR$ molecules that feature large substituents. Irrespective of the types of substituents used for the $RTl \equiv PR$ species, the theoretical investigations (based on the natural bond orbital, the natural resonance theory, and the charge decomposition analysis) demonstrate that their $Tl \equiv P$ triple bonds are very weak. However, the theoretical results predict that only bulkier substituents greatly stabilize the triply bonded $RTl \equiv PR$ species, from the kinetic viewpoint.

Keywords: triply bonded molecules; triple bond; acetylene; substituent effects

1. Introduction

The preparation and characterization of triply bonded heavier main group element (E_{14} = Si, Ge, Sn, and Pb) molecules (i.e., $RE_{14} \equiv E_{14}R$) is a popular field of study in inorganic chemistry [1–41]. From the valence electron viewpoint, the triply bonded $RE_{13} \equiv E_{15}R$ compound is isoelectronic to the $RE_{14} \equiv E_{14}R$ species. However, the former has been the subject of much less study than the latter, in the field of synthetic chemistry. Therefore, the level of understanding of the chemistry of $RE_{13} \equiv E_{15}R$ is lower than that for group 14 less-coordinate alkyne analogues.

In the group 15 family, phosphorus is more similar to its diagonal relative, carbon, than to nitrogen [42]. Thallium is also known to be monovalent and has an ionic radius that is similar to that of potassium, so it is often presumed to be a pseudo alkali metal [43]. The isolation and characterization of the singly bonded organothallium phosphorus molecule, $(Me_3SiCH_2)_3Tl–P(SiMe_3)_3$, was experimentally reported about twenty years ago [44]. Two other novel compounds that contain the thallium–phosphorus single bond have also been identified [45,46]. If both thallium and phosphorus elements could be stabilized using a single bond to connect them, it might be possible to extend this field to the study of other triply bonded $RTl \equiv PR$ inorganic molecules. This work reports the first theoretical study of the possible synthesis of the $RTl \equiv PR$ molecule, which may be isolable as a long-lived compound. The study determines potential inorganic complexes that can stabilize

the thallium≡phosphorus triple bond, to demonstrate the theoretical possibility that these unusual acetylene inorganic analogues can be synthesized.

2. Methodology

Using the Gaussian 09 program package [47], all geometries are fully optimized at the M06-2X [48], B3LYP [49,50], and B3PW91 [51,52] levels of theory, in conjunction with the Def2-TZVP [53] and LANL2DZ+dp [54–58] basis sets. These DFT calculations are signified as M06-2X/Def2-TZVP, B3PW91/Def2-TZVP and B3LYP/LANL2DZ+dp, respectively. In order to confirm that the reactants and products have no imaginary frequencies and that the transition states possess only one imaginary frequency, frequency calculations were performed for all structures. Thermodynamic corrections to 298 K, heat capacity corrections and entropy corrections (ΔS) are applied to the three levels of DFT. The relative free energy (ΔG) at 298 K is also computed at the same levels of theory.

Next, (Si*i*PrDis$_2$)Tl≡P(Si*i*PrDis$_2$), (Tbt)Tl≡P(Tbt), and (Ar*)Tl≡P(Ar*) are the model reactants for this study. It is known that the B3LYP functional fails to describe non-valent interactions, such as the London dispersion correctly. As a result, for large ligands, calculations were performed using dispersion-corrected M06-2X method [48]. Because of the limitations of the available memory size and CPU time, frequencies are not computed at the dispersion-corrected M06-2X/Def2-TZVP level of theory for the triply bonded R´Tl≡PR' systems that have bulky ligands (R'), so the zero-point energies and the Gibbs free energies that are derived using the dispersion-corrected M06-2X/Def2-TZVP cannot be used for these systems.

3. General Considerations

Two interaction models that describe the chemical bonding of the triply bonded RTl≡PR, which serve as a basis for discussion, are given in this section. For convenience, the RTl≡PR molecule is divided into two fragments: Tl–R and P–R. On the basis of theoretical results (see below), three computational methods (M06-2X/Def2-TZVP, B3PW91/Def2-TZVP and B3LYP/LANL2DZ+dp) all indicate that the Tl–R and P–R fragments are respectively calculated to be in the singlet ground state and the triplet ground state.

In model [I], electron promotion energy (ΔE_1) forces the P–R moiety from the triplet ground state to the singlet excited state, so the electronic structure of RTl≡PR can be described in terms of the dimerization of singlet Tl–R and singlet P–R fragments, as shown in Figure 1. From the chemical bonding viewpoint, model [I] shows that the Tl≡P triple bond consists of one σ–donation of Tl→P and two π–donations of Tl←P. In model [II], the electron advancement energy (ΔE_2) promotes the Tl–R unit from the singlet ground state to the triplet excited state. Accordingly, the bonding structure of RTl≡PR can also be represented as the dimerization of triplet Tl–R and triplet P–R fragments, as shown in Figure 1. From the bonding structure viewpoint, model [II] shows that the Tl≡P triple bond is composed of one Tl←P π–bond, one regular σ–bond and one π–bond.

It is schematically shown in Figure 1 that the formation of the triply bonded RTl≡PR molecule can be regarded as either [Tl–R]^1 + [P–R]^1 → [RTl≡PR]^1 (model [I]) or [Tl–R]^3 + [P–R]^3 → [RTl≡PR]^1 (model [II]). It is worthy of note that since the lone pair of phosphorus has significant amount of s character, this could reduce the bonding overlaps between Tl and P elements (see the black lines in model [I] and model [II] in Figure 1). As a consequence, the Tl≡P triple bond should be very weak, which is in contrast to the traditional triple bond of acetylene. This prediction is confirmed in the following section. Both models are used in this study clearly show that the Tl≡P triple bond is mostly attributed to electron donation from the lone pair of P to the empty p-orbital of Tl.

This bonding analysis is used to interpret the bonding properties of the triply bonded RTl≡PR molecule in the next section.
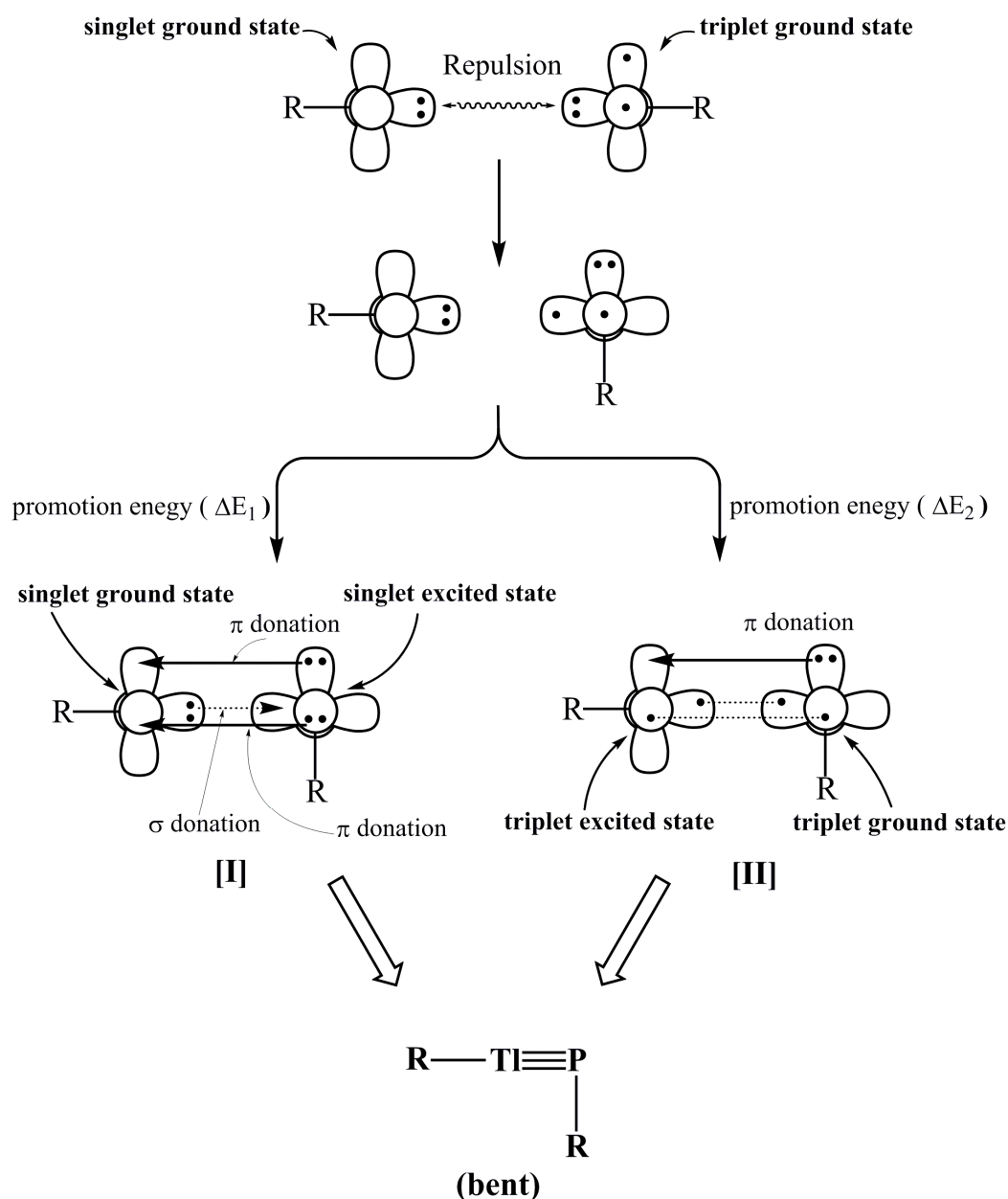
Figure 1. The interaction models, [I] and [II], for the triply bonded RTl≡PR molecule.

4. Results and Discussion

4.1. Small Ligands on Substituted RTl≡PR

The effect of small substituents on the stability of the triply bonded RTl≡PR species is discussed from the kinetic and the thermodynamic viewpoints. Five small substituents (R = H, F, OH, CH_3 and SiH_3) are used for the RTl≡PR model molecule. The important geometrical parameters for the RTl≡PR compounds are calculated at the three computational methods (M06-2X/Def2-TZVP, B3PW91/Def2-TZVP and B3LYP/LANL2DZ+dp) and the results are listed in Table 1. The Cartesian coordinates for the triply bonded minima are given in the Supplementary Information.

Table 1. The important geometrical parameters, the natural charge densities (Q_{Tl} and QP), the binding energies (BE), the HOMO-LUMO energy gaps and the Wiberg Bond Index (WBI) for RTl≡PR using the M06-2X/Def2-TZVP, B3PW91/Def2-TZVP (in round brackets) and B3LYP/LANL2DZ+dp (in square brackets) levels of theory.

R	F	OH	H	CH₃	SiH₃
Tl≡P (Å)	2.422 (2.425) [2.455]	2.437 (2.443) [2.480]	2.320 (2.327) [2.331]	2.339 (2.349) [2.360]	2.313 (2.336) [2.337]
R-P-Tl (°)	179.7 (179.7) [178.5]	179.1 (176.5) [177.9]	179.1 (178.5) [178.2]	175.2 (174.5) [171.3]	174.6 (175.7) [179.1]
P-Tl-R (°)	94.63 (96.59) [94.22]	98.92 (101.5) [100.1]	86.51 (86.82) [86.36]	100.4 (102.2) [102.6]	94.76 (92.71) [90.78]
R-P-Tl-R (°)	180.0 (180.0) [180.0]	179.4 (178.8) [179.2]	179.1 (179.2) [179.8]	178.0 (178.8) [179.9]	177.0 (179.1) [179.4]
Q_P [1]	0.16 (0.17) [0.096]	0.076 (0.13) [0.021]	−0.63 (−0.60) [−0.62]	−0.37 (−0.33) [−0.39]	−0.83 (−0.72) [−0.76]
Q_Tl [2]	1.19 (1.11) [1.25]	1.14 (1.03) [1.17]	1.12 (0.87) [0.99]	1.07 (0.99) [1.13]	0.82 (0.75) [0.89]
ΔE_ST for Tl–R (kcal/mol) [3]	102.1 (103.7) [102.2]	83.57 (80.69) [83.15]	84.85 (85.69) [83.05]	66.82 (67.38) [67.94]	75.96 (77.63) [74.40]
ΔE_ST for P–R (kcal/mol) [4]	−28.91 (−33.35) [−31.76]	−17.53 (−21.29) [−20.24]	−30.75 (−35.49) [−33.16]	−26.43 (−30.26) [−29.21]	−15.84 (−18.68) [−14.46]
HOMO—LUMO (kcal/mol)	184.1 (131.6) [182.5]	167.6 (118.1) [169.1]	210.6 (212.0) [215.4]	151.2 (149.3) [146.5]	142.1 (145.1) [148.5]
BE (kcal/mol) [5]	95.58 (95.74) [93.43]	83.57 (82.10) [83.15]	84.85 (85.69) [83.05]	66.82 (67.38) [67.94]	75.96 (77.63) [74.40]
WBI [6]	1.159 (1.194) [1.191]	1.162 (1.197) [1.178]	1.456 (1.491) [1.475]	1.382 (1.415) [1.403]	1.404 (1.417) [1.372]

[1] The natural charge density on the central phosphorus atom; [2] The natural charge density on the central thallium atom; [3] ΔE_{ST} (kcal mol⁻¹) = E(triplet state for R–Tl) − E(singlet state for R–Tl); [4] ΔE_{ST} (kcal mol⁻¹) = E(triplet state for R–P) − E(singlet state for R–P); [5] BE (kcal mol⁻¹) = E(singlet state for R–Tl) + E(triplet state for R–P) − E(singlet for RTl≡PR); [6] The Wiberg bond index (WBI) for the Tl≡P bond: see reference [59–61].

There are four noteworthy features of Table 1:

(1) The central Tl≡P triple bond distances (Å) for R = F, OH, H, CH₃ and SiH₃ are respectively estimated to be 2.313–2.422 Å, 2.336–2.443 Å and 2.331–2.480 Å, at the M06-2X/Def2-TZVP, B3PW91/Def2-TZVP and B3LYP/LANL2DZ+dp levels of theory. As mentioned in the Introduction, neither experimental nor theoretical results for the triply bonded RTl≡PR species are available to allow a definitive comparison. However, to the author's best knowledge, there are only a few published reports concerning the singly bonded R₃Tl–PR₃ molecules and these report the Tl–P bond length to be 2.922 Å [44], 3.246–3.301 Å [45] and 3.032–3.168 Å [46]. These single bond distances are all longer than the sum of the covalent radii (i.e., 2.62 Å) [62] for the Tl and P elements.

(2) The three DFT calculations shown in Table 1 demonstrate that the R–Tl and R–P components have a singlet and triplet ground state, respectively. The three DFT computational results also show that the singlet-triplet energy differences (ΔE_{ST}) for R–Tl and R–P fragments are estimated to be at

least +67 and −15 kcal/mol, respectively. These energy values strongly suggest that model [I], which is shown in Figure 1, is superior to model [II] in describing the bonding characters of triply bonded RTl≡PR molecules that feature small substituents (R). Model [I] shows that the bonding structure of the triple bond in RTl≡PR can be represented as Tl⇆P. It must be noted that the fact that the lone pair of phosphorus has s character and the valence p orbital of phosphorus is much smaller than that of thallium means that both factors can vigorously affect the bonding overlaps between phosphorus and thallium atoms. Therefore, it is anticipated that the triple bond in these RTl≡PR species is very weak. This prediction is confirmed by the three DFT calculations shown in Table 1. All of the values for the Wiberg bond index (WBI) [59–61] are a little bit higher than 1.0, rather than 2.0. That is to say, regardless of whether small electropositive or small electronegative groups are attached, the RTl≡PR systems possess a quite weak Tl≡P triple bond.

(3) As already shown, model [I] describes the bonding characters in triply bonded RTl≡PR compounds that feature small substituents better than model [II]. This, in turn, strongly implies that an acute bond angle ∠Tl–P–R (close to 90°) and a linear bond angle ∠R–Tl–P (close to 180°) is favored in the triply bonded RTl≡PR molecule, which is verified by the three DFT calculations as shown in Table 1. The nearly perpendicular angle on the P center can also be attributed to the "orbital non-hybridization effect" [63–66] and the "inert *s*-pair effect" [63–66] as discussed previously.

(4) The binding energies (BE) that are required to cleave the central Tl≡P bond, which leads to one R–Tl and one R–P fragment in the singlet ground state and in the triplet ground state, respectively, are summarized in Table 1. The calculated BE values (kcal/mol) for the RTl≡PR molecules are in the range of 67–96, 67–96 and 68–93, at the M06-2X, B3PW91 and B3LYP levels of theory, respectively. This data confirms that the central thallium and phosphorus atoms in the substituted RTl≡PR compounds are strongly bonded.

Considering the stability of RTl≡PR, the theoretical results for the potential energy surfaces of the model molecule, RTlPR (R = F, OH, H, CH_3 and SiH_3), are described in Figure 2. This figure shows a number of stationary points exist, including local minima that correspond to RTl≡PR, R_2Tl=P, Tl=PR_2 and the transition states that connect them. The three DFT computational results show that all of the triply bonded RTl≡PR compounds that feature small substituents immediately transfer to the corresponding doubly bonded species via facile 1,2-migration reactions. In other words, the theoretical evidence shows that triply bonded RTl≡PR species that feature small ligands are both kinetically and thermodynamically unstable, regardless of whether they are electronegative or electropositive, so it is unlikely that they could be prepared or synthesized in a laboratory.

4.2. Large Ligands on Substituted R′Tl≡PR′

As previously mentioned, in order to stabilize R′Tl≡PR′ from the kinetic viewpoint, three types of large substituents (R′) are used in this study. These are SiMe(Si*t*Bu$_3$)$_2$, Si*i*PrDis$_2$, Tbt (=C_6H_2-2,4,6-(CH(SiMe$_3$)$_2$)$_3$), and Ar* (=C_6H_3-2,6-(C_6H_2-2,4,6-*i*-Pr$_3$)$_2$) [67,68], as shown in Figure 3. The geometrical structures of R′Tl≡PR′ are optimized at the dispersion-corrected M06-2X/Def2-TZVP [53] level of theory. Their important calculated parameters are listed in Table 2.

Table 2. The Bond Lengths (Å), Bond Angels (°), Singlet—Triplet Energy Splitting (Δ*E*ST), Natural Charge Densities (QTl and QP), Binding Energies (BE), the HOMO-LUMO Energy Gaps, the Wiberg bond index (WBI), and Some Reaction Enthalpies for R′Tl≡PR′ at the dispersion-corrected M06-2X/Def2-TZVP Level of Theory. See also Figure 4.

R′	SiMe(Si*t*Bu$_3$)$_2$	Si*i*PrDis$_2$	Tbt	Ar*
Tl≡P (Å)	2.386	2.384	2.385	2.336
∠R′–Tl–P (°)	166.9	166.4	168.9	161.2
∠Tl–P–R′ (°)	122.3	113.7	116.2	115.6
∠R′–Tl–P–R′ (°)	171.4	179.5	173.9	174.4
Q_{Tl} [1]	0.975	0.739	1.166	1.218

Table 2. *Cont.*

R′	SiMe(Si*t*Bu₃)₂	Si*i*PrDis₂	Tbt	Ar*
Q$_P$ [2]	−0.860	−0.826	−0.344	−0.257
ΔE$_{ST}$ for Tl—R′ (kcal/mol) [3]	35.91	35.52	31.27	30.24
ΔE$_{ST}$ for P—R′ (kcal/mol) [4]	−43.10	−37.47	−39.74	−40.52
HOMO—LUMO (kcal/mol)	71.27	27.21	58.05	39.34
BE (kcal/mol) [5]	80.24	85.43	62.51	67.89
ΔH$_1$ (kcal/mol) [6]	91.34	90.49	89.22	87.11
ΔH$_2$ (kcal/mol) [6]	73.98	72.83	71.27	74.01
WBI [7]	2.116	2.273	2.127	2.201

[1] The natural charge density on the central thallium atom; [2] The natural charge density on the central phosphorus atom; [3] ΔE$_{ST}$ (kcal mol⁻¹) = E(triplet state for R′–Tl) – E(singlet state for R′–Tl); [4] ΔE$_{ST}$ (kcal mol⁻¹) = E(triplet state for R′–P) – E(singlet state for R′–P); [5] BE (kcal mol⁻¹) = E(triplet state for R′–Tl) + E(singlet state for R′–P) – E(singlet for R′Tl≡PR′); [6] See Figure 4; [7] The Wiberg bond index (WBI) for the Tl≡P bond: see reference [59–61].
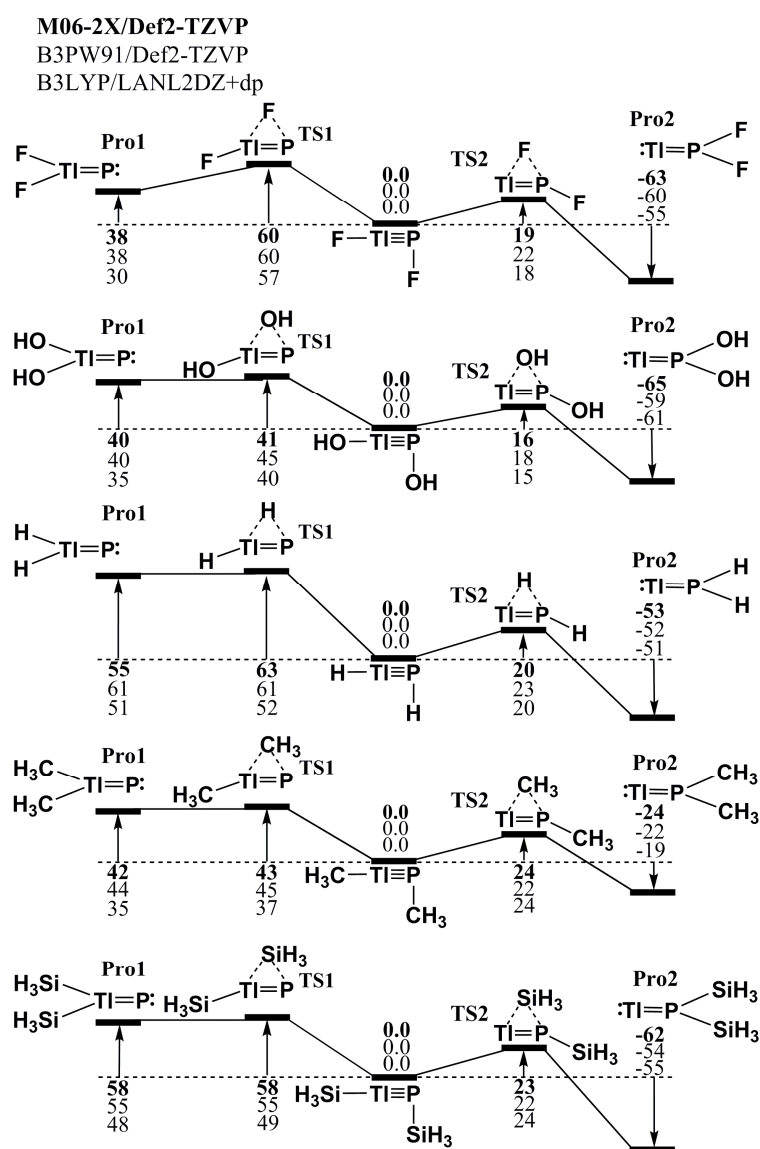

Figure 2. The Relative Gibbs free energy surfaces for RTl≡PR (R = F, OH, H, CH3 and SiH3). These energies are in kcal/mol and are calculated at the M06-2X/Def2-TZVP, B3PW91/Def2-TZVP, and B3LYP/LANL2DZ+dp levels of theory. For details see the text and Table 1.
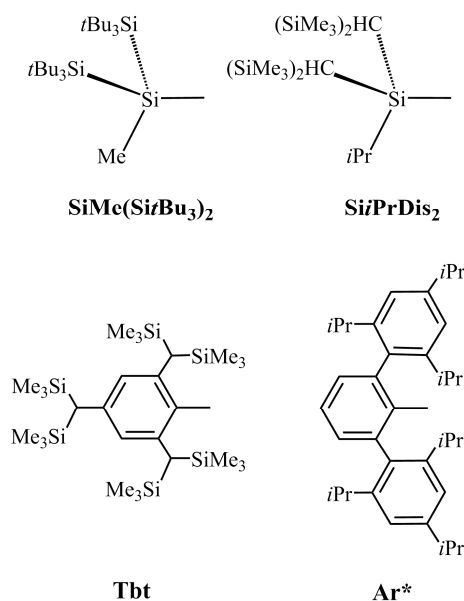
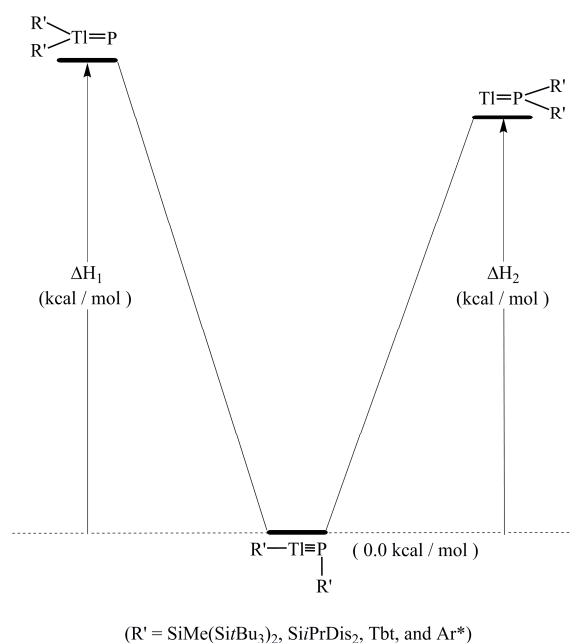**Figure 3.** Four bulky groups. For details, see references [66,67].

(R' = SiMe(Si*t*Bu$_3$)$_2$, Si*i*PrDis$_2$, Tbt, and Ar*)

Figure 4. The potential energy surface for the 1,2-migration reaction of the R'Tl≡PR' molecules with balky groups (R').

Five important conclusions can be drawn from these theoretical results:

(i) The results presented in Table 2 predict that the Tl≡P triple bond lengths (Å) are about 2.386 Å, 2.384 Å, 2.385 Å, and 2.336 Å, for (SiMe(Si*t*Bu$_3$)$_2$)Tl≡P(SiMe(Si*t*Bu$_3$)$_2$), (Si*i*PrDis$_2$)Tl≡P(Si*i*PrDis$_2$), (Tbt)Tl≡P(Tbt), and (Ar*)Tl≡P(Ar*), respectively. These theoretically estimated values are shorter than the experimentally reported Tl–P single bond distance, as mentioned previously [44–46]. Similarly to the case for small substituents, the DFT optimized results show that all of the triply bonded R'Tl≡PR' molecules that feature bulky ligands studied adopt a bent structure, as shown in Table 2.

(ii) If the R'Tl≡PR' compound is cut in half, the Tl–R' and P–R' two fragments are obtained. The DFT results shown in Table 2 demonstrate that the ΔE_{ST} for the Tl–R' unit is greater than 30 kcal/mol

and the modulus of ΔE_{ST} for the P–R′ moiety is greater than 37 kcal/mol. That is to say, the promotion energy from the singlet ground state to the triplet excited for Tl–R′ is smaller than the energy that is required for promotion from that for Tl–R (Table 1). The bonding model that is shown in Figure 1 shows that model [II] can be used to interpret the bonding character in triply bonded R′Tl≡PR′ molecules that feature bulky ligands, R′. Namely, the bonding structure of the triple bond in R′Tl≡PR′ is best described as Tl≦P. In this model, the electrons that are donated from the lone pair of phosphorus have s character, as shown in Figure 1. Moreover, the size of 2p orbital of P is also much smaller than the 6p orbital of Tl. These two factors combined produce a weak Tl≡P triple bond in the R′Tl≡PR′ species. Supporting theoretical evidence in Table 2 shows that the WBI for R′Tl≡PR′ is 2.21, 2.37, 2.13, and 2.20 for R = SiMe(SitBu$_3$)$_2$, SiiPrDis$_2$, Tbt, and Ar*, respectively. These WBI values are much smaller than the value for acetylene (2.99).

(iii) In order to determine the effect of bulky substituents on the stability of triply bonded R′Tl≡PR′ compounds, the dispersion-corrected M06-2X/Def2-TZVP level of theory is used to determine the potential energy surfaces for the isomerization reaction. As shown in Table 2, the triply bonded R′Tl≡PR′ molecules have values that are at least 87 (ΔH_1) and 71 (ΔH_2) kcal/mol lower than that for the corresponding doubly bonded isomers. Therefore, the theoretical results show that a triply bonded R′Tl≡PR′ compound that features bulky substituents is more stable than its corresponding doubly bonded R′$_2$Tl=P: and: Tl=PR′$_2$ isomers, from the kinetic viewpoint.

(iv) In order to verify the conclusion from point (ii), "charge decomposition analysis" (CDA), reported by Dapprich and Frenking [69] is used in the present study. For instance, the computational results concerning (SiMe(SitBu$_3$)$_2$)Tl≡P(SiMe(SitBu$_3$)$_2$) based on the dispersion-corrected M06-2X/Def2-TZVP method are collected in Table 3. As seen in the X column, the biggest contribution from R′–Tl to R′–P is No.227 (HOMO–1) orbital. However, the largest contribution from R′–P to R′–Tl is No.228 (HOMO) orbital. As a result, the net electron transfer (−0.213) is from R′–P to R′–Tl, which is shown in the (X − Y) column. Namely, the R′–P unit donates more electrons to the R′–Tl unit. The theoretical evidence is in good agreement with the valence-electron bonding model (Figure 1; model [II]) as stated earlier. Consequently, the bonding nature of R′Tl≡PR′ can be considered as R′Tl≦PR′.

(v) The NBO [59–61] and NRT [70–72] are also used to determine the bonding properties of the electronic structures of the R′Tl≡PR′ molecules, as shown in Table 4. This table clearly shows that the major bonding character between Tl and P comes from electron donation from 2p(P) to 6p(Tl), which is denoted as 6p(Tl) ← 2p(P). In the (SiMe(SitBu$_3$)$_2$)Tl≡P(SiMe(SitBu$_3$)$_2$) molecule, for instance, the dispersion-corrected M06-2X/Def2-TZVP calculations show that the Tl≡P π bonding occurs as follows: $\pi_\perp$ (Tl≡P) = 0.3114(sp$^{4.77}$)Tl + 0.9503(sp$^{1.42}$)P. That is, a polarized $\pi_\perp$ bond exists between Tl and P, which arises from the donation of the P lone pair to the empty Tl p orbital. As seen in Table 4, the Tl≡P $\pi_\perp$ bonding orbitals comprise 9.7% natural Tl orbitals and 90% natural P orbitals (Figure 5). The similar theoretical results can also be found in the Tl≡P $\pi_\parallel$ bonding orbitals as already represented in Table 4.
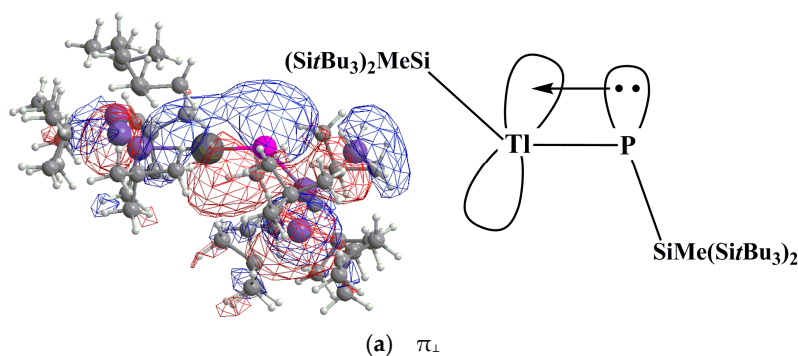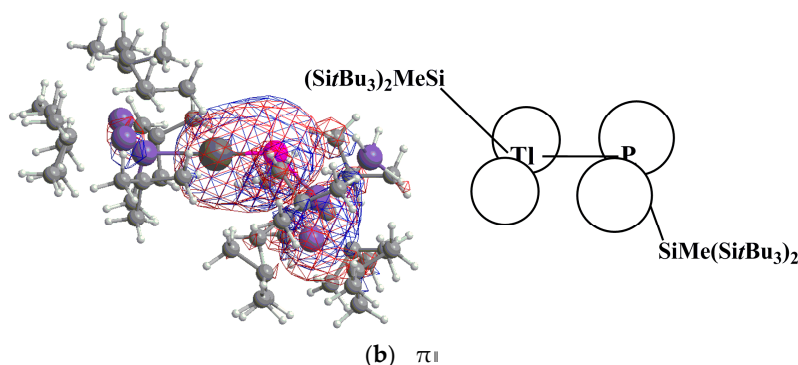

(a) $\pi_\perp$

Figure 5. *Cont.*

(b) $\pi_\parallel$

Figure 5. The natural Tl≡P π bonding orbitals ((**a**) and (**b**)) for (SiMe(Si*t*Bu₃)₂)Tl≡P(SiMe(Si*t*Bu₃)₂). For comparison, see also Figure 3.

Table 3. The charge decomposition analysis (CDA) [a] for R′Tl≡PR′ (R′ = SiMe(Si*t*Bu₃)₂) system based on M06-2X orbitals, where the X term indicates the number of electrons donated from R′–Tl fragment to R′–P fragment, the Y term indicates the number of electrons back donated from R′–P fragment to R′–Tl fragment and the Q term indicates the number of electrons involved in repulsive polarization. Significant X and Y terms are bolded for easier comparison. [a],[b]

	Orbital	Occupancy	X	Y	X − Y	Q
	218	2.000000	0.000757	0.000586	0.000171	−0.002462
	219	2.000000	0.001036	0.000522	0.000513	−0.004450
	220	2.000000	0.000932	0.000539	0.000394	−0.006342
	221	2.000000	0.000026	0.004350	−0.004325	−0.002504
	222	2.000000	0.001151	−0.000164	0.001315	−0.001354
	223	2.000000	0.000081	0.003145	−0.003064	−0.001960
	224	2.000000	0.000037	0.002403	−0.002366	−0.000054
	225	2.000000	0.001777	0.029263	−0.027486	−0.030329
	226	2.000000	0.000477	0.013735	−0.013259	−0.007124
	227	2.000000	0.008445	0.068258	−0.059813	−0.018272
HOMO	228	2.000000	−0.005339	0.003033	−0.008432	−0.004437
LUMO	229	0.000000	0.000000	0.000000	0.000000	0.000000
	230	0.000000	0.000000	0.000000	0.000000	0.000000
sum		456.000000	0.028853	0.241774	−0.212922	−0.107250

[a] For clearness, only list the X, Y, and Q terms for HOMO (No.228) –10 ~LUMO+2. [b] Summation of contributions from all unoccupied and occupied orbitals.

Table 4. The natural bond orbital (NBO) and the natural resonance theory (NRT) analysis for R′Tl≡PR′ molecules that feature ligands (R′ = SiMe(Si*t*Bu₃)₂, Si*i*PrDis₂, Tbt, and Ar*) at the dispersion-corrected M06-2X/Def2-TZVP level of theory [1,2].

R′Tl≡PR′	WBI	NBO Analysis			NRT Analysis	
		Occupancy	Hybridization	Polarization	Total/Covalent/Ionic	Resonance Weight
R′ = SiMe(Si*t*Bu₃)₂	2.11	σ = 2.21	σ : 0.5116 Tl (sp$^{1.27}$) + 0.8592 P (sp$^{2.07}$)	26.18% (Tl) 73.82% (P)	2.22/1.55/0.67	Tl–P: 23.17% Tl=P: 66.87% Tl≡P: 9.94%
		$\pi_\perp$ = 1.84	$\pi_\perp$: 0.3114 Tl (sp$^{4.77}$) + 0.9503 P (sp$^{1.42}$)	9.70% (Tl) 90.30% (P)		
		$\pi_\parallel$ = 1.92	$\pi_\parallel$: 0.6833 Tl (sp$^{99.87}$) + 0.7556 P (sp$^{99.99}$)	5.69% (Tl) 94.31% (P)		
R′ = Si*i*PrDis₂	2.37	σ = 1.83	σ : 0.6422 Tl (sp$^{0.86}$) + 0.7665 P (sp$^{20.18}$)	41.24% (Tl) 58.76% (P)	2.59/0.83/1.76	Tl–P: 17.35% Tl=P: 71.14% Tl≡P: 11.51%
		$\pi_\perp$ = 1.92	$\pi_\perp$: 0.4064 Tl (sp$^{99.99}$) + 0.9137 P (sp$^{44.72}$)	16.51% (Tl) 83.49% (P)		
		$\pi_\parallel$ = 1.93	$\pi_\parallel$: 0.4551 Tl (sp$^{99.99}$) + 0.8997 P (sp$^{94.99}$)	14.79% (Tl) 85.21% (P)		

Table 4. *Cont.*

R′Tl≡PR′	WBI	NBO Analysis			NRT Analysis	
		Occupancy	Hybridization	Polarization	Total/Covalent/Ionic	Resonance Weight
R′ = Tbt	2.13	σ = 1.77	σ: 0.6888 Tl (sp$^{0.94}$) + 0.7249 P (sp$^{38.46}$)	47.45% (Tl) 52.55% (P)	2.08/1.59/0.49	Tl–P: 27.42% Tl=P: 63.76% Tl≡P: 8.82%
		$\pi_\perp$ = 1.94	$\pi_\perp$: 0.4133 Tl (sp$^{35.51}$) + 0.9244 P (sp$^{87.83}$)	23.43% (Tl) 82.74% (P)		
		$\pi_\parallel$ = 1.90	$\pi_\parallel$: 0.4118 Tl (sp$^{99.89}$) + 0.9077 P (sp$^{99.99}$)	17.28% (Tl) 82.72% (P)		
R′ = Ar*	2.20	σ = 1.96	σ: 0.7362 Tl (sp$^{0.04}$) + 0.6767 P (sp$^{64.96}$)	54.20% (Tl) 45.80% (P)	2.17/1.66/0.51	Tl–P: 19.82% Tl=P: 71.69% Tl≡P: 8.49%
		$\pi_\perp$ = 1.77	$\pi_\perp$: 0.3177 Tl (sp$^{99.99}$) + 0.9482 P (sp$^{99.99}$)	10.09% (Tl) 89.91% (P)		
		$\pi_\parallel$ = 1.92	$\pi_\parallel$: 0.4083 Tl (sp$^{99.99}$) + 0.9128 P (sp$^{99.99}$)	16.67% (Tl) 83.33% (P)		

[1] The value of the Wiberg bond index (WBI) for the Tl–P bond and the occupancy of the corresponding σ and π bonding NBO (see reference [59–61]). [2] NRT; see reference [70–72].

5. Conclusions

In summary, the theoretical observations strongly support the idea that both electronic and steric effects determine the relative stability of molecules that contain a Tl≡P triple bond, as well as its corresponding doubly bonded isomers. The simple bonding models schematically illustrated in Figure 1 show that model [I], whose bonding character is symbolized by Tl⇆P, better interprets the triple bond in RTl≡PR species that feature small substituents. Model [II], whose bonding property is typified as Tl≡P, better describes the triple bond in R′Tl≡PR′ molecules that feature bulky ligands (Figure 6). However, regardless of whether the substituents in triply bonded RTl≡PR compound are large or small, their Tl≡P triple bonds are quite weak. Two effects can explain these phenomena. The different sizes of the p orbitals in the Tl and P elements mean that their overlapping populations are pretty small and the lone pair of the phosphorus atom has significant amount of s character, which results in poor overlaps between thallium and phosphorus. It is hoped that the results of experimental synthesis and structural characterization will confirm these predictions.
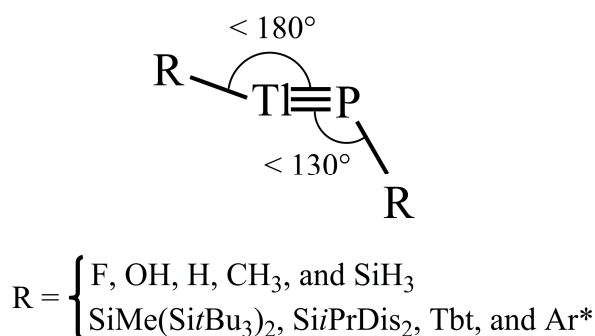

$$R = \begin{cases} F,\ OH,\ H,\ CH_3,\ and\ SiH_3 \\ SiMe(SitBu_3)_2,\ SiiPrDis_2,\ Tbt,\ and\ Ar* \end{cases}$$

Figure 6. The predicted geometrical structure based on the present theoretical calculations.

References

1. Bino, A.; Ardon, M.; Shirman, E. Formation of a carbon-carbon triple bond by coupling reactions in aqueous solution. *Science* **2005**, *308*, 234–235. [CrossRef] [PubMed]

2. Su, P.; Wu, J.; Gu, J.; Wu, W.; Shaik, S.; Hiberty, P.C. Bonding conundrums in the C_2 molecule: A valence bond study. *J. Chem. Theory Comput.* **2011**, *7*, 121–130. [CrossRef] [PubMed]

3. Ploshnik, E.; Danovich, D.; Hiberty, P.C.; Shaik, S. The nature of the idealized triple bonds between principal elements and the σ origins of trans-bent geometries—A valence bond study. *J. Chem. Theory Comput.* **2011**, *7*, 955–968. [CrossRef] [PubMed]

4. Danovich, D.; Bino, A.; Shaik, S. Formation of carbon–carbon triply bonded molecules from two free carbyne radicals via a conical intersection. *J. Phys. Chem. Lett.* **2013**, *4*, 58–64. [CrossRef] [PubMed]

5. Power, P.P. π-Bonding and the lone pair effect in multiple bonds between heavier main group elements. *Chem. Rev.* **1999**, *99*, 3463–3504. [CrossRef] [PubMed]

6. Jutzi, P. Stable systems with a triple bond to silicon or its homologues: Another challenge. *Angew. Chem. Int. Ed.* **2000**, *39*, 3797–3800. [CrossRef]

7. Weidenbruch, M. Some recent advances in the chemistry of silicon and its homologues in low coordination states. *J. Organomet. Chem.* **2002**, *646*, 39–52. [CrossRef]

8. Power, P.P. Silicon, germanium, tin and lead analogues of acetylenes. *Chem. Commun.* **2003**, 2091–2101. [CrossRef]

9. Weidenbruch, M. Molecules with a genuine Si-Si triple bond and a stable derivative of $[SiH]^+$. *Angew. Chem. Int. Ed.* **2005**, *44*, 514–516. [CrossRef] [PubMed]

10. Power, P.P. Synthesis and some reactivity studies of germanium, tin and lead analogues of alkynes. *Appl. Organomet. Chem.* **2005**, *19*, 488–493. [CrossRef]

11. Lein, M.; Krapp, A.; Frenking, G. Why do the heavy-atom analogues of acetylene E_2H_2 (E = Si$-$Pb) exhibit unusual structures? *J. Am. Chem. Soc.* **2005**, *127*, 6290–6299. [CrossRef] [PubMed]

12. Sekiguchi, A.; Ichinohe, M.; Kinjo, R. The chemistry of disilyne with a genuine Si–Si triple bond: Synthesis, structure, and reactivity. *Bull. Chem. Soc. Jpn.* **2006**, *79*, 825–828. [CrossRef]

13. Power, P.P. Bonding and reactivity of heavier group 14 element alkyne analogues. *Organometallics* **2007**, *26*, 4362–4366. [CrossRef]

14. Sekiguchi, A. Disilyne with a silicon-silicon triple bond: A new entry to multiple bond chemistry. *Pure Appl. Chem.* **2008**, *80*, 447–451. [CrossRef]

15. Sekiguchi, A.; Kinjo, R.; Ichinohe, M. Interaction of π-bonds of the silicon–silicon triple bond with alkali metals: An isolable anion radical upon reduction of a disilyne. *Synt. Met.* **2009**, *159*, 773–780. [CrossRef]

16. Fischer, R.C.; Power, P.P. π-Bonding and the lone pair effect in multiple bonds involving heavier main group elements: Developments in the new millennium. *Chem. Rev.* **2010**, *110*, 3877–3882. [CrossRef] [PubMed]

17. Peng, Y.; Fischer, R.C.; Merrill, W.A.; Fischer, J.; Pu, L.; Ellis, B.D.; Fettinger, J.C.; Herber, R.H.; Power, P.P. Substituent effects in ditetrel alkyne analogues: Multiple vs. single bonded isomers. *Chem. Sci.* **2010**, *1*, 461–478. [CrossRef]

18. Sasamori, T.; Han, J.S.; Hironaka, K.; Takagi, N.; Nagase, S.; Tokitoh, N. Synthesis and structure of stable 1,2-diaryldisilyne. *Pure Appl. Chem.* **2010**, *82*, 603–611. [CrossRef]

19. Sekiguchi, A.; Kinjo, R.; Ichinohe, M. A stable compound containing a silicon–silicon triple bond. *Science* **2004**, *305*, 1755–1758. [CrossRef] [PubMed]

20. Wiberg, N.; Vasisht, S.K.; Fischer, G.; Mayer, P.Z. Disilynes. III [1] a relatively stable disilyne RSi≡SiR (R = SiMe(Si*t*Bu₃)₂). *Anorg. Allg. Chem.* **2004**, *630*, 1823–1831. [CrossRef]

21. Sasamori, T.; Hironaka, K.; Sugiyama, T.; Takagi, N.; Nagase, S.; Hosoi, Y.; Furukawa, Y.; Tokitoh, N. Synthesis and reactions of a stable 1,2-diaryl-1,2-dibromodisilene: A precursor for substituted disilenes and a 1,2-diaryldisilyne. *J. Am. Chem. Soc.* **2008**, *130*, 13856–13868. [CrossRef] [PubMed]

22. Stender, M.; Phillips, A.D.; Wright, R.J.; Power, P.P. Synthesis and characterization of a digermanium analogue of an alkyne. *Angew. Chem. Int. Ed.* **2002**, *41*, 1785–1789. [CrossRef]

23. Stender, M.; Phillips, A.D.; Power, P.P. Formation of [Ar*Ge{CH₂C(Me)C(Me)CH₂}CH₂C(Me)=]₂ (Ar* = C₆H₃-2,6-Trip₂; Trip = C₆H₂-2,4,6-*i*-Pr₃) via reaction of Ar*GeGeAr* with 2,3-dimethyl-1,3-butadiene: Evidence for the existence of a germanium analogue of an alkyne. *Chem. Commun.* **2002**, 1312–1313. [CrossRef]

24. Pu, L.; Phillips, A.D.; Richards, A.F.; Stender, M.; Simons, R.S.; Olmstead, M.M.; Power, P.P. Germanium and tin analogues of alkynes and their reduction products. *J. Am. Chem. Soc.* **2003**, *125*, 11626–11632. [CrossRef] [PubMed]

25. Sugiyama, Y.; Sasamori, T.; Hosoi, Y.; Furukawa, Y.; Takagi, N.; Nagase, S.; Tokitoh, N. Synthesis and properties of a new kinetically stabilized digermyne: New insights for a germanium analogue of an alkyne. *J. Am. Chem. Soc.* **2006**, *128*, 1023–1031. [CrossRef] [PubMed]

26. Spikes, G.H.; Power, P.P. Lewis base induced tuning of the Ge–Ge bond order in a "digermyne". *Chem. Commun.* **2007**, 85–88. [CrossRef] [PubMed]

27. Phillips, A.D.; Wright, R.J.; Olmstead, M.M.; Power, P.P. Synthesis and characterization of 2,6-Dipp$_2$-H$_3$C$_6$SnSnC$_6$H$_3$-2,6-Dipp$_2$ (Dipp = C$_6$H$_3$-2,6-Pr$^i_2$): A tin analogue of an alkyne. *J. Am. Chem. Soc.* **2002**, *124*, 5930–5931. [CrossRef] [PubMed]

28. Pu, L.; Twamley, B.; Power, P.P. Synthesis and characterization of 2,6-Trip$_2$H$_3$C$_6$PbPbC$_6$H$_3$-2,6-Trip$_2$ (Trip = C$_6$H$_2$-2,4,6-*i*-Pr$_3$): A stable heavier group 14 element analogue of an alkyne. *J. Am. Chem. Soc.* **2000**, *122*, 3524–3525. [CrossRef]

29. Karni, M.; Apeloig, Y.; Schröder, D.; Zummack, W.; Rabezzana, R.; Schwarz, H. Nachweis von HCSiF und HCSiCl als die ersten Moleküle mit formalen C≡Si-Bindungen. *Angew. Chem. Int. Ed.* **1999**, *38*, 332–335.

30. Danovich, D.; Ogliaro, F.; Karni, M.; Apeloig, Y.; Cooper, D.L.; Shaik, S. Silynes (RC identical with SiR′) and disilynes (RSi identical with SiR′): Why are less bonds worth energetically more? *Angew. Chem. Int. Ed.* **2001**, *40*, 4023–4027. [CrossRef]

31. Gau, D.; Kato, T.; Saffon-Merceron, N.; Cozar, A.D.; Cossio, F.P.; Baceiredo, A. Synthesis and structure of a base-stabilized C-phosphino-Si-amino silyne. *Angew. Chem. Int. Ed.* **2010**, *49*, 6585–6589. [CrossRef] [PubMed]

32. Lühmann, N.; Müller, T. A compound with a Si-C triple bond. *Angew. Chem. Int. Ed.* **2010**, *49*, 10042–10046. [CrossRef] [PubMed]

33. Liao, H.-Y.; Su, M.-D.; Chu, S.-Y. A stable species with a formal Ge≡C triple bond–a theoretical study. *Chem. Phys. Lett.* **2001**, *341*, 122–131. [CrossRef]

34. Wu, P.-C.; Su, M.-D. The effect of substituents on the stability of triply bonded galliumuantimony molecules: A new target for synthesis. *Dalton. Trans.* **2011**, *40*, 4253–4260. [CrossRef] [PubMed]

35. Wu, P.-C.; Su, M.-D. Triply bonded stannaacetylene (RC≡SnR): Theoretical designs and characterization. *Inorg. Chem.* **2011**, *50*, 6814–6822. [CrossRef] [PubMed]

36. Wu, P.-C.; Su, M.-D. A new target for synthesis of triply bonded plumbacetylene (RC≡PbR): A theoretical design. *Organometallics* **2011**, *30*, 3293–3303. [CrossRef]

37. Paetzold, P. Iminoboranes. *Adv. Inorg. Chem.* **1987**, *31*, 123–132.

38. Paetzold, P. Boron Chemistry. In Proceedings of the 6th International Meeting on Born Chemistry, Bechyne, Slovakia, 22–26 June 1987; Hermanek, S., Ed.; World Scientific: Singapore, 1987; p. 446.

39. Paetzold, P. New perspectives in boron-nitrogen chemistry-I. *Pure Appl. Chem.* **1991**, *63*, 345–363. [CrossRef]

40. Paetzold, P. Boron-Nitrogen analogues of cyclobutadiene, benzene and cyclooctatetraene: Interconversions. *Phosphorus Sulfur Silicon Relat. Elem.* **1994**, *93*, 39–50. [CrossRef]

41. Wright, R.J.; Phillips, A.D.; Allen, T.L.; Fink, W.H.; Power, P.P. Synthesis and characterization of the monomeric imides Ar′MNAr″ (M = Ga or In; Ar′ or Ar″ = terphenyl ligands) with two-coordinate gallium and indium. *J. Am. Chem. Soc.* **2003**, *125*, 1694–1696. [CrossRef] [PubMed]

42. Dillon, K.B.; Mathey, F.; Nixon, J.F. *Phosphorus: The Carbon Copy: From Organophosphorus to Phospha-Organic Chemistry*; Wiley: New York, NY, USA, 1998; p. 2.

43. Mosha, D.M.S. The monomeric pentacyanocobaltate (II) anion: Preparation and properties of thallium (I) pentacyanocobaltate (II). *J. Chem. Educ.* **1982**, *59*, 1057–1068. [CrossRef]

44. Baldwin, R.A.; Wells, R.L.; White, P.S. Synthesis and characterization of an organothallium-phosphorus adduct: Crystal structure of (Me$_3$SiCH$_2$)$_3$Tl·P(SiMe$_3$)$_3$. *Main Group Chem.* **1997**, *2*, 67–75. [CrossRef]

45. Francis, M.D.; Jones, C.; Deacon, G.B.; Delbridge, E.E. Synthesis and structural characterization of a novel polyheterocyclopentadienyl thallium (I) complex. *Organometallics* **1998**, *17*, 3826–3832. [CrossRef]

46. Fox, A.R.; Wright, R.J.; Rivard, E.; Power, P.P. Tl$_2$[Aryl$_2$P$_4$]: A thallium complexed diaryltetraphosphabutadienediide and its two-electron oxidation to a diaryltetraphosphabicyclobutane, Aryl$_2$P$_4$. *Angew. Chem. Int. Ed.* **2005**, *44*, 7729–7733. [CrossRef] [PubMed]

47. Frisch, M.J.; Trucks, G.W.; Schlegel, H.B.; Scuseria, G.E.; Robb, M.A.; Cheeseman, J.R.; Scalmani, G.; Barone, V.; Mennucci, B.; Petersson, G.A.; et al. *Gaussian 09*, version Revision D.01; Gaussian, Inc.: Wallingford, CT, USA, 2013.

48. Zhao, Y.; Truhlar, D.G. Density functionals with broad applicability in chemistry. *Acc. Chem. Res.* **2008**, *41*, 157–167. [CrossRef] [PubMed]

49. Becke, A.D. Density-Functional exchange-energy approximation with correct asymptotic behavior. *Phys. Rev. A* **1988**, *38*, 3098–3100. [CrossRef]

50. Becke, A.D. Density-Functional thermochemistry. *J. Chem. Phys.* **1993**, *98*, 5648–5652. [CrossRef]

51. Lee, C.; Yang, W.; Parr, R.G. Development of the Colle-Salvetti correlation-energy formula into a functional of the electron density. *Phys. Rev. B* **1988**, *37*, 785–789. [CrossRef]

52. Perdew, J.P.; Wang, Y. Accurate and simple analytic representation of the electron-gas correlation energy. *Phys. Rev.* **1992**, *B45*, 13244–13249. [CrossRef]

53. Weigend, F.; Ahlrichs, R. Balanced basis sets of split valence, triple zeta valence and quadruple zeta valence quality for H to Rn: Design and assessment of accuracy. *Phys. Chem. Chem. Phys.* **2005**, *7*, 3297–3305. [CrossRef] [PubMed]

54. Dunning, T.H., Jr.; Hay, P.J. *Modern Theoretical Chemistry*; Schaefer, H.F., III, Ed.; Plenum: New York, NY, USA, 1976; pp. 1–28.

55. Hay, P.J.; Wadt, W.R. *Ab initio* effective core potentials for molecular calculations. Potentials for the transition metal atoms Sc to Hg. *J. Chem. Phys.* **1985**, *82*, 270–283. [CrossRef]

56. Hay, P.J.; Wadt, W.R. *Ab initio* effective core potentials for molecular calculations. Potentials for main group elements Na to Bi. *J. Chem. Phys.* **1985**, *82*, 284–298.

57. Hay, P.J.; Wadt, W.R. *Ab initio* effective core potentials for molecular calculations. Potentials for K to Au including the outermost core orbitals. *J. Chem. Phys.* **1985**, *82*, 299–310. [CrossRef]

58. Check, C.E.; Faust, T.O.; Bailey, J.M.; Wright, B.J.; Gilbert, T.M.; Sunderlin, L.S. Addition of polarization and diffuse functions to the LANL2DZ basis set for p-block elements. *J. Phys. Chem. A* **2001**, *105*, 8111–8116. [CrossRef]

59. The Wiberg Bond Index, Which is Used to Screen Atom Pairs for the Possible Bonding in the Natural Bonding Orbital (NBO) Search, are Performed with the NBO Program (version NBO 6.0; University of Wisconsin System: Madison, WI, USA, 2013). Available online: http://www.chem.wisc.edu/~nbo5 (accessed on 4 July 2017).

60. Wiberg, K.B. Application of the pople-santry-segal CNDO method to the cyclopropylcarbinyl and cyclobutyl cation and to bicyclobutane. *Tetrahedron* **1968**, *24*, 1083–1096. [CrossRef]

61. Reed, A.E.; Curtiss, L.A.; Weinhold, F. Intermolecular interactions from a natural bond orbital, donor-acceptor viewpoint. *Chem. Rev.* **1998**, *88*, 899–993. [CrossRef]

62. Emsley, J. *The Elements*, 2nd ed.; Clarendon Press: Oxford, UK, 1991; p. 285.

63. Pyykko, P.; Desclaux, J.-P. Relativity and the periodic system of elements. *Acc. Chem. Res.* **1979**, *12*, 276–282. [CrossRef]

64. Kutzelnigg, W. Chemical bonding in higher main group elements. *Angew. Chem. Int. Ed. Engl.* **1984**, *23*, 272–276. [CrossRef]

65. Pyykko, P. Relativistic effects in structural chemistry. *Chem. Rev.* **1988**, *88*, 563–623. [CrossRef]

66. Pyykko, P. Strong closed-shell interactions in inorganic chemistry. *Chem. Rev.* **1997**, *97*, 597–636. [CrossRef] [PubMed]

67. Kobayashi, K.; Nagase, S. Silicon−Silicon triple bonds: Do substituents make disilynes synthetically accessible? *Organometallics* **1997**, *16*, 2489–2495. [CrossRef]

68. Kobayashi, K.; Takagi, N.; Nagase, S. Do bulky aryl groups make stable silicon−silicon triple bonds synthetically accessible? *Organometallics* **2001**, *20*, 234–236. [CrossRef]

69. Dapprich, S.; Frenking, G. Investigation of donor-acceptor interactions: A charge decomposition analysis using fragment molecular orbitals. *J. Phys. Chem.* **1995**, *99*, 9352–9367. [CrossRef]

70. Glendening, E.D.; Weinhold, F. Natural resonance theory: I. General formalism. *J. Comput. Chem.* **1998**, *19*, 593–606. [CrossRef]

71. Glendening, E.D.; Weinhold, F. Natural resonance theory: II. Natural bond order and valency. *J. Comput. Chem.* **1998**, *19*, 610–623. [CrossRef]

72. Glendening, E.D.; Weinhold, F.; Badenhoop, J.K. Natural resonance theory. III. Chemical applications. *J. Comput. Chem.* **1998**, *19*, 628–632. [CrossRef]

Sample Availability: Not available.